

# Effects of different alkalis on the behaviour of vanadium loss in the pretreatment of vanadium-bearing acid leaching solution

Qiaoqiao Zheng<sup>a,b</sup>, Yimin Zhang<sup>a,b,c,d,\*</sup>, Shenxu Bao<sup>a,b</sup>, Jing Huang<sup>c,d</sup>, Guobin Zhang<sup>a,b</sup>

<sup>a</sup> School of Resources and Environmental Engineering, Wuhan University of Technology, Wuhan 430070, China

<sup>b</sup> Hubei Key Laboratory of Mineral Resources Processing and Environment, Wuhan 430070, China

<sup>c</sup> State Environmental Protection Key Laboratory of Mineral Metallurgical Resources Utilization and Pollution Control, Wuhan University of Science and Technology, Wuhan 430081, China

<sup>d</sup> Hubei Collaborative Innovation Centre for High Efficient Utilization of Vanadium Resources, Wuhan University of Science and Technology, Wuhan 430081, China

\*Corresponding author, e-mail: zym126135@126.com

Received 8 Jun 2018

Accepted 3 Feb 2019

**ABSTRACT:** This study examined the effect of different pretreating agents on vanadium loss from vanadium-bearing shale. Acid leaching solutions with added  $\text{Ca}(\text{OH})_2$ ,  $\text{CaCO}_3$ ,  $\text{NaOH}$ ,  $\text{Na}_2\text{CO}_3$ , and ammonia solution were evaluated. The pH of the acid leaching solution was adjusted to 2.0 to reduce vanadium loss and allow efficient removal of impurities, providing a high vanadium extraction efficiency.  $\text{Ca}(\text{OH})_2$  was the most effective neutralizer and its use resulted in a vanadium loss rate as low as 4%. SEM-EDS analysis indicates that a major cause of vanadium loss is entrapment and absorption by precipitates. The low vanadium loss rate using  $\text{Ca}(\text{OH})_2$  as a neutralizer appears to be due to the smooth and flat surface of the precipitate, which limits vanadium entrainment. When the pH was adjusted with  $\text{CaCO}_3$ , the crystal structure of the precipitate was incomplete. In addition,  $\text{CaSO}_4$  and iron phosphate particles interact, promoting entrainment and absorption of vanadium. Similarly, flocculent iron phosphate was generated when the pH was adjusted with  $\text{NaOH}$ ,  $\text{Na}_2\text{CO}_3$ , or ammonia, resulting in a crystal with a rough surface that easily entrained vanadium.

**KEYWORDS:** vanadium, acid leaching solution, pH adjustment, alkali

## INTRODUCTION

Vanadium is a vital rare element that is widely used in high-tech fields, including the production of redox batteries and aerospace<sup>1</sup>, due to its special physical and chemical properties<sup>2,3</sup>. In China, the major source of vanadium is vanadium-bearing shale<sup>4-6</sup>. High salt roasting-water leaching, blank roasting-acid leaching, blank roasting-alkali leaching, and direct acid leaching<sup>7-9</sup> have been used to recover vanadium from vanadium-bearing shale. Among these processes, roasting- $\text{H}_2\text{SO}_4$  leaching has received considerable attention for extraction of vanadium-bearing shale due to its highest recovery rate<sup>10</sup>. However, impurities, such as Fe, P, and other elements, can be leached along with vanadium in the acid leaching process. This results in a complex, low pH mixture with the vanadium-containing extract contaminated with high concentrations of

impurities. These conditions prevent efficient vanadium separation and concentration<sup>11-13</sup>.

At present, the main methods for vanadium separation and concentration are solvent extraction<sup>14-16</sup> and ion exchange<sup>17,18</sup>. The solvent extraction method, with various extracting reagents, has gradually been the primary methods due to its high efficiency with no requirement for complex equipment<sup>19</sup>. Among the reagents used for vanadium extraction, the acid extractant D2EHPA (Bis(2-ethylhexyl) phosphate) provides advantages of acid system adaptability and easy stripping<sup>20-22</sup>. The appropriate pH range for solvent extraction of vanadium is 1.5–2.5; however, the acidity of the acid leaching solution is often excessive, requiring pretreated to allow subsequent steps in the extraction process<sup>23,24</sup>. Some methods for the disposal of acid leaching solution have also been developed, these include ion exchange, solvent extraction, and

**Table 1** Chemical composition of acid leaching solutions (g/l).

Element	V	Fe	Na	Ca	Al	P	S	Si
Conc.	3.10	1.66	1.91	1.11	3.81	1.25	29.1	1.48

alkali neutralization<sup>25–27</sup>. Although ion exchange and solvent extraction can purify the acid leaching solution, the pH of treated solution does not meet the requirements for the next step in the extraction process<sup>28</sup>. Hence neutralization with alkali is a popular and necessary process to adjust the pH of acid leaching solution before subsequent extraction<sup>29,30</sup>. Currently, NaOH is used to adjust pH; however, this results in considerable vanadium loss and introduces many impurities.

In this study, Ca(OH)<sub>2</sub>, CaCO<sub>3</sub>, NaOH, Na<sub>2</sub>CO<sub>3</sub>, and ammonia were used to adjust the pH of vanadium-bearing shale acid leaching solution. The mechanisms of vanadium loss and the introduction of impurities during precipitation under different alkalis condition were investigated by XRD and SEM-EDS. Furthermore, the vanadium loss rate, removal rate of impurity ions, and vanadium extraction efficiency were evaluated to select the appropriate alkali and pH for the pretreatment process.

## MATERIALS AND METHODS

Vanadium-bearing shale was supplied by Ping-fan Mining Co. Ltd., Zaoyang, China. The acid leaching solution from vanadium-bearing shale was prepared by heating vanadium-bearing shale at 850 °C for 1.5 h followed by leaching with 5% (wt) CaF<sub>2</sub> and 15% (v/v) H<sub>2</sub>SO<sub>4</sub> solution (L/S= 1.5:1) at 98 °C for 2 h. The chemical composition of the acid leaching solution is shown in Table 1 and the initial pH was 0.33. Na<sub>2</sub>SO<sub>3</sub> was used to reduce the vanadium(V) and iron(III) to vanadium(IV) and iron(II). Analytical grade Ca(OH)<sub>2</sub>, CaCO<sub>3</sub>, NaOH, Na<sub>2</sub>CO<sub>3</sub>, and NH<sub>3</sub>·H<sub>2</sub>O were obtained from Shanghai Rare-Earth Chemical Co., Ltd., China. The extracting solution was composed of 5% (v/v) TBP (tributyl phosphate), 20% (v/v) P204 (Bis(2-ethylhexyl) phosphate D2EHPA), and 75% (v/v) sulfonated kerosene. P204 and TBP were purchased from Sinopharm Chemical Reagent Co., Ltd., China. All other reagents used were of analytical grade.

The vanadium concentration in solution was measured indirectly using iron ammonium sulphate titration, with the iron concentration determined colorimetrically using 1,10-phenanthroline. The concentrations of other ions in the solution were de-

termined using inductively coupled plasma-optical emission spectroscopy (ICP-OES, Optima 4300DV, Perkin-Elmer, USA). The mineralogical composition of the neutralizing filtered residue was identified by XRD spectra pattern, recorded with a D/MAX 2500PC X-ray powder diffractometer (Rigaku, Japan) at room temperature. Microscopic observation and elemental analysis (SEM with EDS) were conducted using a JEOL JSM-6610 scanning electronic microscope (JEOL, Japan) equipped with a BRUKER QUANTAX 200-30 energy dispersive spectrometer (BRUKER, Germany). The pH of the solution was measured with a PHS-3C digital pH meter (Shanghai Rex Instruments Factory, China).

The pH adjustment experiments were carried out using a magnetic stirrer. In each pH adjustment experiment, 100 ml acid leaching solution was reduced with Na<sub>2</sub>SO<sub>3</sub> for 30 min. The pH of the solutions was then adjusted with Ca(OH)<sub>2</sub>, CaCO<sub>3</sub>, NaOH, Na<sub>2</sub>CO<sub>3</sub>, or NH<sub>3</sub>·H<sub>2</sub>O. After pH adjustment, the solutions were filtered and washed for a selected duration, preparing the feed solution for solvent extraction. The solvent extraction was performed by magnetically stirred with the organic and aqueous phases at a 1:2 ratio, for 8 min at 25 °C in a water bath. Phase separation was achieved by gravity using separatory funnels. After phase separation, the ion concentrations in the raffinate were determined with the concentration of ions in organic phase deduced from mass-balance calculations. The distribution ratio (*D*) and extraction efficiency (*E*) were calculated by  $D = C_{\text{org}}/C_{\text{aq}}$  and  $E = D/[D + (V_{\text{aq}}/V_{\text{org}})] \times 100\%$ , respectively, where *C*<sub>org</sub> is the concentration of vanadium presented in the organic phase, *C*<sub>aq</sub> is the content of vanadium in the raffinate, and *V*<sub>aq</sub> and *V*<sub>org</sub> are the volumes of aqueous and organic phases used in the extraction, respectively.

## RESULTS AND DISCUSSION

### Effects of pH on ion precipitation

To determine the optimal pH in the neutralization process, the effect of pH on vanadium loss and removal of impurity ions was investigated. Ca(OH)<sub>2</sub>, CaCO<sub>3</sub>, NaOH, Na<sub>2</sub>CO<sub>3</sub>, and NH<sub>3</sub>·H<sub>2</sub>O were used as alkali neutralizers to adjust the pH of acid leaching solution from 1.4–2.4. The results shown in Fig. 1 indicate that the solution pH is a factor that substantially influences the vanadium loss rate and impurity ion removal efficiency. The vanadium loss rate and impurity ion (Fe, Al, P, S) removal efficiency increases as pH increases; however, the

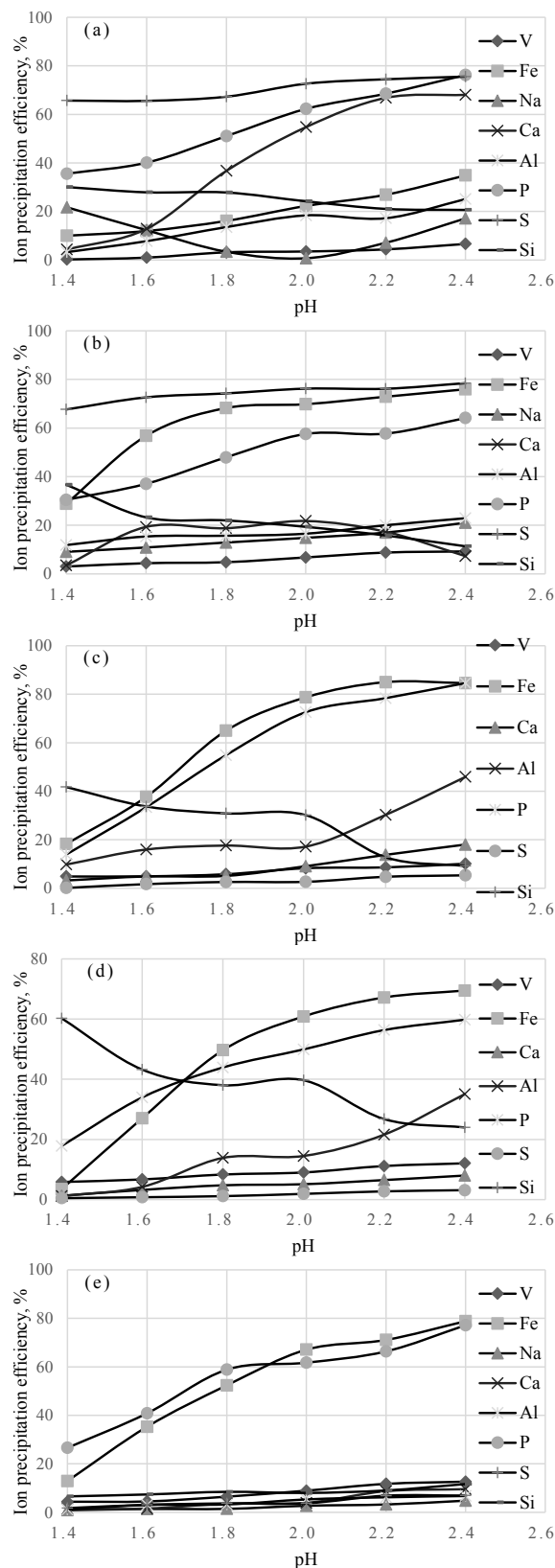


**Fig. 1** Effect of pH on ion precipitation when adjusting pH with: (a) Ca(OH)<sub>2</sub>, (b) CaCO<sub>3</sub>, (c) NaOH, (d) Na<sub>2</sub>CO<sub>3</sub>, and (e) NH<sub>3</sub>·H<sub>2</sub>O.

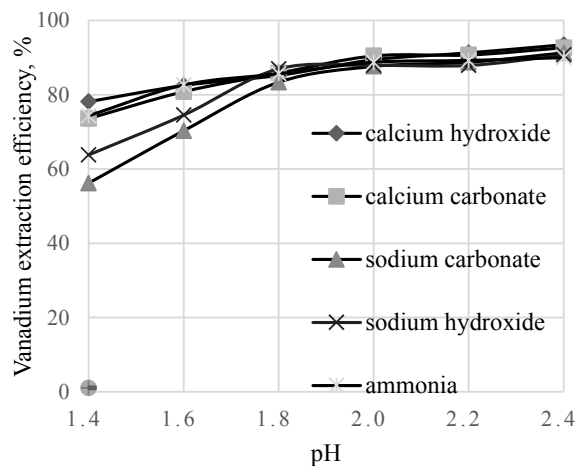


**Fig. 2** Effect of pH on vanadium extraction using different alkali neutralizers.

removal efficiency of Si decreases as pH increases. The removal efficiency of Fe and P increases as pH increases. As shown in Fig. 1a,b, when pH was adjusted with Ca(OH)<sub>2</sub> and CaCO<sub>3</sub>, the removal rate of S was enhanced 60%, this may be due to the generation of CaSO<sub>4</sub> from dissolved Ca(OH)<sub>2</sub> and CaCO<sub>3</sub>. Possible chemical reactions are described in Table 4(1,2).

As shown in Fig. 1c,d, when the pH was adjusted with NaOH and Na<sub>2</sub>CO<sub>3</sub>, the removal efficiency of Si sharply decreases as pH increases from 2.0–2.2. When pH was adjusted with NH<sub>3</sub>·H<sub>2</sub>O, vanadium loss rate and impurity ion (Al, S, Na, Ca) removal efficiency increases as pH increases slightly, however, the removal efficiency of Fe and P increases as pH increases significantly (Fig. 1e).

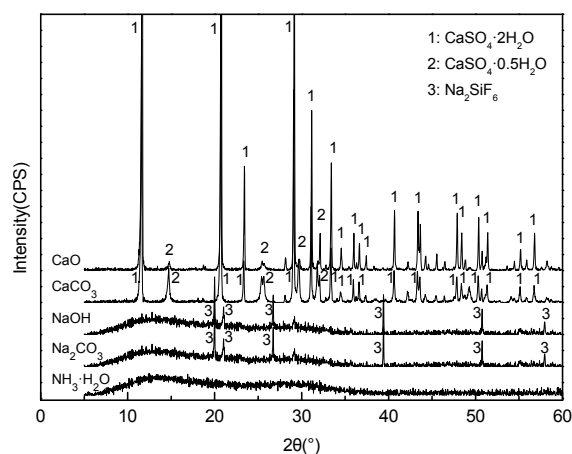
Based on the experiments described above, we conclude that the removal efficiency of P and Fe increases significantly when pH increases, however, the vanadium loss rate also increases. Hence the optimal pH range was determined to be 1.8–2.2 to promote precipitation of less vanadium and more impurities.

**Effects of pH on vanadium extraction**

The effect of pH on vanadium extraction efficiency was also investigated. Solution extraction experiments were carried out under the following conditions: contact time, 8 min; temperature, 25 °C; and organic to aqueous phase ratio (O/A), 1:2. Under these conditions, the extraction efficiency of vanadium increases as pH increases (Fig. 2). When pH was greater than 2.0, the extraction of vanadium was almost constant even with further increases in

**Table 2** The ion precipitation efficiency with pH adjusted to 2.0 (%).

Alkali	Element							
	V	Fe	Na	Ca	Al	P	S	Si
Ca(OH) <sub>2</sub>	3.5	54.8	22.3	0.8	18.4	62.3	72.6	27.8
CaCO <sub>3</sub>	6.8	69.8	14.8	21.8	16.6	57.6	76.2	19.4
NaOH	8.3	78.7	–	7.1	17.2	72.6	2.7	30.2
Na <sub>2</sub> CO <sub>3</sub>	9.0	60.7	–	6.5	22.5	50.9	1.9	39.7
NH <sub>3</sub> ·H <sub>2</sub> O	8.9	67.1	2.7	3.9	5.3	61.7	3.8	8.0

**Fig. 3** XRD pattern of precipitate when pH was adjusted with alkalis.

pH. Hence the optimal pH for acid leaching solution was 2.0.

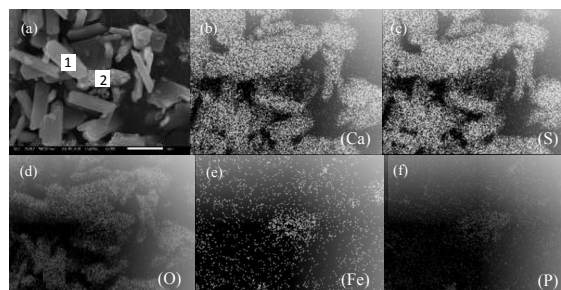
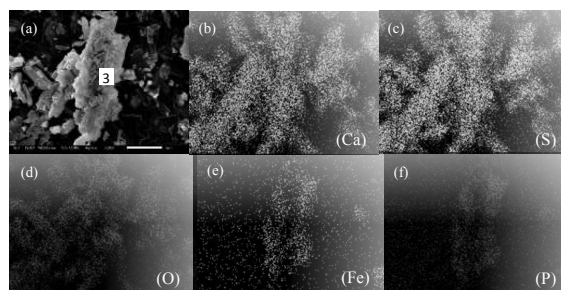
#### Comparison of different alkali neutralizers

Alkali neutralizers, to adjust the pH of the acid leaching solution, were investigated with regard to vanadium loss rate and impurity ion removal efficiency. The lowest vanadium loss rate, 4%, and efficient removal of other impurity ions was achieved with Ca(OH)<sub>2</sub> used to adjust pH (Table 2). When the pH was adjusted with Ca(OH)<sub>2</sub> and CaCO<sub>3</sub>, the number of calcium ions generated was relatively small. However, using NaOH and Na<sub>2</sub>CO<sub>3</sub> as alkali neutralizers, a large amount of Na ions was produced. The use of NH<sub>3</sub>·H<sub>2</sub>O resulted in the generation of ammonia nitrogen wastewater, which is difficult to treat. Considering the above factors, the best alkali neutralizer for the neutralization process was determined to be Ca(OH)<sub>2</sub>.

#### XRD and SEM-EDS analysis

##### pH adjustment with Ca(OH)<sub>2</sub> and CaCO<sub>3</sub>

XRD and SEM-EDS were used to analyse precipitates generated after adjusting pH to 2.0 to determine

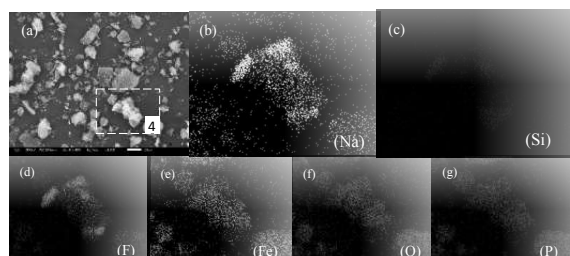
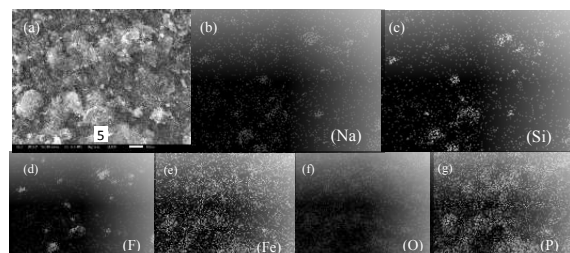
**Fig. 4** (a) SEM image of precipitate when pH was adjusted with Ca(OH)<sub>2</sub>, EDS elemental distribution: (b) Ca; (c) S; (d) O; (e) Fe; (f) P**Fig. 5** (a) SEM image of precipitate when pH was adjusted with CaCO<sub>3</sub>, EDS elemental distribution: (b) Ca; (c) S; (d) O; (e) Fe; (f) P

the mechanism of vanadium loss. When Ca(OH)<sub>2</sub> and CaCO<sub>3</sub> were used to adjust pH, the major components of the precipitate were CaSO<sub>4</sub>·2H<sub>2</sub>O and CaSO<sub>4</sub>·0.5H<sub>2</sub>O (Fig. 3). The SEM-EDS electronic images from precipitates formed when adjusting the pH with Ca(OH)<sub>2</sub> indicates the presence of prismatic gypsum crystals with surfaces that are smooth and flat, limiting the potential for vanadium to be entrained (Fig. 4). The type of crystal structure formed with Ca(OH)<sub>2</sub> likely contributes to the lowest vanadium loss rate with this alkali neutralizer. In contrast, the precipitate formed when adjusting pH with CaCO<sub>3</sub> (Fig. 5) exhibits many small gypsum particles stuck together. This crystal structure could more easily intercalate vanadium consistent with the increased loss rate when the pH was adjusted with Ca(OH)<sub>2</sub>.

The EDS elemental distribution reveals that the contribution of O, P and Fe was limited, suggesting that the Fe, P and O might exist in the form of iron phosphate. However, the content of iron phosphate is too low to account for the EDS result, as there is no peak for iron phosphate in the XRD pattern. The result of the EDS spot analysis (Table 3) indicates

**Table 3** EDS spot analysis (labeled boxes 1–6) of precipitates based on Figs. 4–8 (wt%).

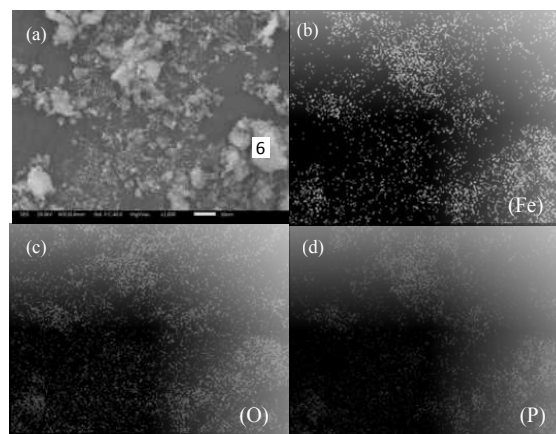
Element	V	Fe	P	O	K	Na	Ca	F	Si	S	Al
1	–	0.69	–	64.44	–	–	18.30	–	–	16.57	–
2	0.57	12.65	7.54	61.60	1.50	–	7.71	–	–	8.39	–
3	0.37	8.88	4.43	46.46	–	–	20.15	–	–	19.10	0.61
4	0.47	22.27	14.43	46.83	0.96	4.52	–	10.26	0.27	–	–
5	1.02	28.81	19.15	45.57	1.49	3.72	0.24	–	–	–	–
6	0.61	17.57	11.42	69.90	0.50	–	–	–	–	–	–

**Fig. 6** (a) SEM image of precipitate when pH was adjusted with NaOH, EDS elemental distribution: (b) Na; (c) Si; (d) F; (e) Fe; (f) O; (g) P**Fig. 7** (a) SEM image of precipitate when pH was adjusted with Na<sub>2</sub>CO<sub>3</sub>, EDS elemental distribution: (b) Na; (c) Si; (d) F; (e) Fe; (f) O; (g) P

that the surface of CaSO<sub>4</sub> crystals does not contain vanadium. However, adherence of small iron phosphate particles to the CaSO<sub>4</sub> surface can promote the absorption of vanadium, resulting in vanadium loss (vanadium content of 0.57% and 0.37%).

#### pH adjustment with NaOH and Na<sub>2</sub>CO<sub>3</sub>

The major component of precipitate when pH was adjusted with NaOH was Na<sub>2</sub>SiF<sub>6</sub> (Fig. 3). When dissolved NaOH and Na<sub>2</sub>CO<sub>3</sub> released Na<sup>+</sup>, which reacted with SiF<sub>6</sub><sup>2-</sup> in the acid leaching solution generating Na<sub>2</sub>SiF<sub>6</sub><sup>31</sup>. However, the large number of dispersion peaks in the XRD pattern indicates poor crystallization of sodium fluorosilicate. Possible chemical reaction equations are shown in

**Fig. 8** (a) SEM image of precipitate when pH was adjusted with NH<sub>3</sub>·H<sub>2</sub>O, EDS elemental distribution: (b) Fe; (c) O; (d) P**Table 4(3,4)**

The results of SEM-EDS (Fig. 6 and Fig. 7) indicate that sodium fluorosilicate crystals are incomplete and covered with floccule. The precipitate surface structure allows for vanadium to be entrained at higher levels compared with Ca(OH)<sub>2</sub> and CaCO<sub>3</sub> as alkali neutralizers. Meanwhile, the floccule consists of O, P and Fe suggesting the presence of iron phosphate. When the pH was adjusted with Na<sub>2</sub>CO<sub>3</sub>, the floccule surface was rougher, entraining more vanadium than when using NaOH. The result of EDS spot analysis shows the vanadium content was 0.47% and 1%, indicating that the iron phosphate entrained and absorbed vanadium, resulting in vanadium loss (Table 3).

#### pH adjustment with NH<sub>3</sub>·H<sub>2</sub>O

The XRD diffraction pattern of precipitate when pH was adjusted with NH<sub>3</sub>·H<sub>2</sub>O was a dispersion peak, indicating that the residue was an amorphous material (Fig. 3). The results of SEM-EDS electronic image and elemental distribution (Fig. 8) reveal

**Table 4**  $\Delta^\circ G(298K)/\text{kJ}\cdot\text{mol}^{-1}$  of reaction equations.

Reaction equations	$\Delta^\circ G(298K)$
1. $\text{Ca}(\text{OH})_2 + 2\text{H}^+ + (\text{SO}_4)^{2-} = \text{CaSO}_4 \downarrow + 2\text{H}_2\text{O}$	-156.8
2. $\text{CaCO}_3 + 2\text{H}^+ + (\text{SO}_4)^{2-} = \text{CaSO}_4 \downarrow + \text{H}_2\text{O} + \text{CO}_2 \uparrow$	-84.2
3. $2\text{NaOH} + 2\text{H}^+ + \text{SiF}_6^{2-} = \text{Na}_2\text{SiF}_6 \downarrow + 2\text{H}_2\text{O}$	-272.5
4. $\text{Na}_2\text{CO}_3 + 2\text{H}^+ + \text{SiF}_6^{2-} = \text{Na}_2\text{SiF}_6 \downarrow + \text{H}_2\text{O} + \text{CO}_2 \uparrow$	-140.9
5. $\text{H}_3\text{PO}_4 + \text{Fe}^{3+} = \text{FePO}_4 \downarrow + 3\text{H}^+$	-46.1
6. $\text{H}_2\text{PO}_4^- + \text{Fe}^{3+} = \text{FePO}_4 \downarrow + 2\text{H}^+$	-27.9

that floccule iron phosphate was formed. Fe can exist as the cation  $\text{Fe}^{3+}$  and P is often present as neutral  $\text{H}_3\text{PO}_4$  and  $\text{H}_2\text{PO}_4^-$ . Possible chemical reactions with  $\text{Fe}^{3+}$ ,  $\text{H}_3\text{PO}_4$  and  $\text{H}_2\text{PO}_4^-$  were described in Table 4(5,6). The result of EDS spot analysis (Table 3) shows that the content of vanadium was 0.61 wt%, indicating that the iron phosphate entrained and absorbed vanadium resulting in vanadium loss.

### Thermodynamics

The feasibility of the reactions described in these equations should be theoretically discussed using thermic analyses. The  $\Delta^\circ G$  (standard free energy change of reaction) can be calculated using the  $^\circ G(T)$  (standard free energy) of the substances involved in the chemical reaction<sup>32</sup>. The functions describing the  $\Delta^\circ G(298K)$  for the reaction equations are shown in Table 4.

Table 4 shows that  $\Delta^\circ G(298K)$  was negative for all reaction equations. Hence all reactions above are spontaneous at 298K.

### CONCLUSIONS

To obtain a low vanadium loss rate, high impurity ions removal rate and high vanadium extraction efficiency, the pH of acid leaching solution should be adjusted to 2.0 with  $\text{Ca}(\text{OH})_2$ .

The mechanism of vanadium loss is that vanadium was entrained and absorbed by precipitate. When adjusting pH with  $\text{Ca}(\text{OH})_2$ , the lowest vanadium loss rate is achieved because crystal structure was the most integrated compared with using other alkalis. When adjusting pH with  $\text{CaCO}_3$ , crystal structure was relatively integrated with tiny calcium sulphate particles stuck together, making it easier to entrain vanadium compared with  $\text{Ca}(\text{OH})_2$ . Meanwhile, the tiny iron phosphate particles adhered to  $\text{CaSO}_4$  surface would entrain and absorb vanadium and result in vanadium loss.

Compared with  $\text{Ca}(\text{OH})_2$ , when NaOH and  $\text{Na}_2\text{CO}_3$  were used to adjust pH, the structure of sodium fluorosilicate was incomplete, and the floccule iron phosphate was produced, which makes the surface rough and causes higher vanadium loss.

When  $\text{NH}_3 \cdot \text{H}_2\text{O}$  was used to adjust pH, amorphous flocculent materials were formed, making it easier to entrain vanadium than when adjusting pH with  $\text{Ca}(\text{OH})_2$ .

**Acknowledgements:** This study was financially supported by the National Natural Science Foundation of China (51774215), the National Natural Science Foundation of China (51874222), and the National Key Science Technology Support Programs of China (2015BAB03B05).

### REFERENCES

- Sun B, Skyllas-Kazacos M (1992) Chemical modification of graphite electrode materials for vanadium redox flow battery application—part II. Acid treatments. *Electrochim Acta* **37**, 2459–65.
- Moskalyk RR, Alfantazi AM (2003) Processing of vanadium: a review. *Miner Eng* **16**, 793–805.
- Nguyen TH, Lee MS (2015) Solvent extraction of vanadium(V) from sulfate solutions using LIX 63 and PC 88A. *J Ind Eng Chem* **31**, 118–23.
- Yimin Z, Shenxu B, Tao L (2011) The technology of extracting vanadium from stone coal in China: history, current status and future prospects. *Hydrometallurgy* **109**, 116–24.
- Zhang G, Zhang Y, Bao S, Huang J, Zhang L (2017) A novel eco-friendly vanadium precipitation method by hydrothermal hydrogen reduction technology. *Minerals* **7**, 182–200.
- Hu P, Zhang Y, Liu T, Huang J, Yuan Y, Xue N (2018) Source separation of vanadium over iron from roasted vanadium-bearing shale during acid leaching via ferric fluoride surface coating. *J Clean Prod* **181**, 399–407.
- Yang Z, Li HY, Yin XC, Yan ZM, Yan XM, Xie B (2014) Leaching kinetics of calcification roasted vanadium slag with high CaO content by sulfuric acid. *Int J Miner Process* **133**, 105–11.
- Choi IH, Kim HR, Moon G, Jyothi RK, Lee JY (2018) Spent  $\text{V}_2\text{O}_5\text{—WO}_3/\text{TiO}_2$  catalyst processing for valuable metals by soda roasting-water leaching. *Hydrometallurgy* **175**, 292–9.
- Nejad DG, Khanchi AR, Taghizadeh M (2018) Recovery of Vanadium from Magnetite Ore Using Direct Acid Leaching: Optimization of Parameters by Plackett-Burman and Response Surface Methodologies. *Jom-US* **70**, 1024–30.
- Aarabi-Karasgani M, Rashchi F, Mostoufi N, Vahidi E (2010) Leaching of vanadium from LD converter slag using sulfuric acid. *Hydrometallurgy* **102**, 14–21.
- Alibrahim M, Shlewit H, Alike S (2008) Solvent extraction of Vanadium (IV) with di(2-ethylhexyl)

- phosphoric acid and tributyl phosphate. *Period Polytech Chem Eng* **52**, 29–33.
12. Li W, Zhang YM, Liu T, Huang J, Wang Y (2013) Comparison of ion exchange and solvent extraction in recovering vanadium from sulfuric acid leach solutions of stone coal. *Hydrometallurgy* **131**, 1–7.
  13. Nikiforova A, Kozhura O, Pasenko O (2017) Application of lime in two-stage purification of leaching solution of spent vanadium catalysts for sulfuric acid production. *Hydrometallurgy* **172**, 51–9.
  14. Xiong P, Zhang Y, Huang J, Bao S, Yang X, Shen C (2017) High-efficient and selective extraction of vanadium (V) with N235-P507 synergistic extraction system. *Chem Eng Res Des* **120**, 284–90.
  15. Tavakoli MR, Dreisinger DB (2014) Separation of vanadium from iron by solvent extraction using acidic and neutral organophosphorus extractants. *Hydrometallurgy* **141**, 17–23.
  16. Xue NN, Zhang YM, Liu T, Huang J, Liu H (2017) Effect of  $K_2SO_4$  on solvent extraction of vanadium with D2EHPA/TBP. *ScienceAsia* **43**, 302–11.
  17. Nguyen TH, Man SL (2013) Separation of molybdenum and vanadium from acid solutions by ion exchange. *Hydrometallurgy* **136**, 65–70.
  18. Kiriya T, Kuroda R (1972) A combined ion-exchange-spectrophotometric determination of vanadium in sea and natural waters. *Anal Chim Acta* **62**, 464–7.
  19. Remya PN, Saji J, Reddy MLP (2004) Extraction and separation of vanadium(V) from multimetal chloride solutions using bis(2,4,4-trimethylpentyl)phosphinic acid. *Solvent Extr Res Dev* **11**, 173–85.
  20. Li X, Wei C, Wu J, Li M, Deng Z, Li C, Xu H (2012) Co-extraction and selective stripping of vanadium (IV) and molybdenum (VI) from sulphuric acid solution using 2-ethylhexyl phosphonic acid mono-2-ethylhexyl ester. *Sep Purif Technol* **86**, 64–9.
  21. Hughes MA, Biswas RK (1991) The kinetics of vanadium (IV) extraction in the acidic sulphate-D2EHPA-n-hexane system using the rotating diffusion cell technique. *Hydrometallurgy* **26**, 281–97.
  22. Noori M, Rashchi F, Babakhani A, Vahidi E (2014) Selective recovery and separation of nickel and vanadium in sulfate media using mixtures of D2EHPA and Cyanex 272. *Sep Purif Technol* **136**, 265–73.
  23. Li X, Wei C, Deng Z, Li M, Li C, Fan G (2011) Selective solvent extraction of vanadium over iron from a stone coal/black shale acid leach solution by D2EHPA/TBP. *Hydrometallurgy* **105**, 359–63.
  24. Yang X, Zhang Y, Bao S (2016) Separation and recovery of sulfuric acid from acidic vanadium leaching solution of stone coal via solvent extraction. *J Environ Chem Eng* **4**, 1399–405.
  25. Nenov V, Dimitrova N, Dobrevsky I (1997) Recovery of sulphuric acid from waste aqueous solutions containing arsenic by ion exchange. *Hydrometallurgy* **44**, 43–52.
  26. Ersöz M (2005) Transport of formic acid through anion exchange membranes by diffusion dialysis and electro-electro dialysis. *Sep Sci Technol* **39**, 165–84.
  27. Shin CH, Kim JY, Kim JY, Kim HS, Lee HS, Mohapatra D, Ahn JW, Ahn JG, B0ae W (2009) Recovery of nitric acid from waste etching solution using solvent extraction. *J Hazard Mater* **163**, 729–34.
  28. Li W, Zhang Y, Huang J, Zhu X, Wang Y (2012) Separation and recovery of sulfuric acid from acidic vanadium leaching solution by diffusion dialysis. *Sep Purif Technol* **96**, 44–9.
  29. Wei C, Li X, Deng Z, Fan G, Li M, Li C (2010) Recovery of  $H_2SO_4$  from an acid leach solution by diffusion dialysis. *J Hazard Mater* **176**, 226–30.
  30. Vitolo S, Seggiani M, Filippi S, Brocchini C (2000) Recovery of vanadium from heavy oil and Orimulsion fly ashes. *Hydrometallurgy* **57**, 141–9.
  31. Liu YH, Yang C, Li PY, Li SQ (2010) A new process of extracting vanadium from stone coal. *Int J Min Met Mater* **17**, 381–8.
  32. Machavaram VR, Badcock RA, Fernando GF (2007) Fabrication of intrinsic fibre Fabry-Perot sensors in silica fibres using hydrofluoric acid etching. *Sens Actuators A Phys* **138**, 248–60.